Vitis **60**, 21–27 (2021) DOI: 10.5073/vitis.2021.60.21-27

High-resolution 3D phenotyping of the grapevine root system using X-ray Computed Tomography

R. Schmitz[1), 3)], B. S. Atkinson[2)], C. J. Sturrock[2)], L. Hausmann[1)], R. Töpfer[1)] and K. Herzog[1)]

[1)] Julius Kühn-Institut, Federal Research Centre for Cultivated Plants, Institute for Grapevine Breeding Geilweilerhof, Siebeldingen, Germany
[2)] Hounsfield Facility, School of Biosciences, University of Nottingham, Leicestershire, United Kingdom
[3)] Institute of Crop Science and Resource Conservation (INRES) - Plant Breeding, University of Bonn, Bonn, Germany

Summary

Plant roots are essential for water and nutrient uptake and contribute to the plants' response to environmental stress factors. As the hidden half of a plant, investigation of root systems is highly challenging, most of available methods are destructive and very labour-intensive. In this proof-of-concept study, a non-invasive X-ray micro computed tomography (X-ray µCT) method was applied to investigate the phenotypic variation of the complex three-dimensional (3D) architecture of grapevine roots as a function of genotype and soil. Woody cuttings of 'Calardis Musqué', 'Villard Blanc' and V3125 ('Schiava Grossa' x 'Riesling') were cultivated in polypropylene columns filled with two different soil types, clay loam and sandy loam, for 6 weeks. Afterwards, the columns were scanned once using the technique of X-ray µCT. The received raw data were analysed for the reconstruction of 3D root system models (3D model), which display a non-destructive visualization of whole, intact root systems with a spatial resolution of 42 µm. The 3D models of all investigated plants (in total 18) were applied to quantify root system characteristics precisely by measuring adventitious root length, lateral root length, total root length, root system surface area, root system volume and root growth angles from the woody cutting relative to a horizontal axis. The results showed that: (i) early root formation and root growth differed between genotypes, especially between 'Calardis Musqué' and 'Villard Blanc'; and (ii) the soil type does influence adventitious root formation of V3125, but had minor effects on 'Calardis Musqué' and 'Villard Blanc'. In conclusion, this innovative, high-resolution method of X-ray µCT is suitable for high resolution phenotyping of root formation, architecture, and rooting characteristics of grapevine woody cuttings in a non-destructive manner, e.g. to investigate root response to drought stress and would provide new insights into phylloxera root infection.

K e y w o r d s : 3D root architecture; 3D root model; non-invasive; X-ray µCT; root angle; root growth; *Vitis vinifera* L.; adventitious root.

Introduction

Grapevines are propagated vegetatively and thus, their root systems emerge from woody, dormant cuttings of canes. Roots arising from woody cuttings are called adventitious roots from which additional lateral roots are branching off. Successful and sufficient rooting ability of grafted grapevines, first growing in nurseries and later in vineyards, depends on the adventitious root formation for water uptake followed by the formation of lateral roots for nutrient uptake. Especially in times of climate change, an increased risk for hot and dry summers can be observed even for cool climate regions like Germany. Root systems that display an efficient water uptake become increasingly important for adaptation to such drought stress periods (Smart *et al.* 2006, Battista *et al.* 2016, Delrot *et al.* 2020).

To meet the challenge for an improved evaluation of breeding material or rootstock varieties growing under different soil conditions and the development of extended selection criteria, sensor-based phenotyping techniques are promising tools e.g. to distinguish between adventitious and lateral root characteristics in an objective, comparable and high-precision way. Recently, most root phenotyping methods applied in vineyards are based on root excavation. The use of a mini excavator (41 mm diameter × 1 m length) allows extracting soil cores with roots at various sites and distances from the trunk (Soar and Loveys 2007). By this, vertical distribution of roots in soil can be observed. Another field approach is root phenotyping by trenching. A one-meter deep trench on one side of the vine row enabled counting of roots and determination of root distribution of 15 to 20 years old grapevines at the section of the trench (Battista *et al.* 2016). Both field phenotyping methods allow investigation of grapevine roots in natural soils but are very labour-intensive and destructive which decreases the number of repetitions. In addition, they suffer from the risk of damaging the roots or (partly) loss of fine root. Furthermore, quantification of roots is limited to a small accessible soil section only, so that an investigation of the three-dimensional (3D) structure of the whole root system is not yet feasible. Non-invasive technologies can be applied to obtain high-resolution 3D information of root architecture. In sugar beet, root-related traits that are relevant for the plant development and yield,

Correspondence to: Dr. K. Herzog, Julius Kühn-Institut (JKI), Federal Research Centre for Cultivated Plants, Institute for Grapevine Breeding Geilweilerhof, 76833 Siebeldingen, Germany. E-mail: katja.herzog@julius-kuehn.de

were monitored non-invasively using magnetic resonance imaging (MRI) (Metzner *et al.* 2014). A combined approach of MRI and positron emission tomography (PET) was utilised to phenotype the root systems of sugar beet, maize and radish based on detection of ^{11}C radioactivity (Jahnke *et al.* 2009). While PET has the advantage of tracing nutrient translocation in the plant, it has a relatively coarse spatial (voxel) resolution of approximately 1.4 mm. Therefore, its value to detect the finely structured lateral roots is limited. In contrast, MRI systems offer a higher spatial resolution of 30 μm^3. Similar spatial resolution (42 µm) is achieved by computed microtomography (X-ray µCT). For investigations of plant samples, vertical sample positioning is preferred but MRI systems are less commonly available with vertical orientated sample loading (*i.e.* a horizontal gantry table in medical systems). Hence, X-ray µCT systems with vertical sample positioning are used more frequently in research laboratories, and in combination with lower equipment costs, their application in plant root research is becoming more and more common (Atkinson *et al.* 2019).

The principle of X-ray µCT technique is based on the differential attenuation of ionising radiation passing through a sample depending on its material density. The number of photons transmitted through the sample is inversely proportional to its density (Mairhofer *et al.* 2015). The system enables non-invasive 3D imaging of whole root systems growing in soil-filled columns and had been applied to study plant-soil interactions of several plant species during the last years, e.g. in rice (Zappala *et al.* 2013) or tomato (Tracy *et al.* 2012). Rogers *et al.* (2016) demonstrated the influence of growth substrates (different kinds of beads, sand and potting soil) on root growth, e.g. total root length is affected by particle size. In addition, a significant interaction was observed between bulk density and soil type to the root volume, root surface, and the total root length of tomato roots (Tracy *et al.* 2012, Helliwell *et al.* 2019). Although root systems of numerous crop species have been scanned and analysed using X-ray µCT, no studies are available applying this technique to investigate grapevine roots regarding their root architecture and root response to different soil types. The texture of the soils hereby is the most important difference (Tab. 1). While clay loam has a fine texture with a higher concentration of silt and clay, sandy loam has a higher concentration of sand, resulting in lower dewatering capacity. Therefore, the present proof-of-concept study aims at: (i) the evaluation of X-ray µCT to acquire the root system of grapevines growing from woody cuttings in a soil pot experiment; (ii) the reconstruction of 3D models by classifying the X-ray µCT data to quantify adventitious and lateral root characteristics non-invasively and with high-resolution; and (iii) evaluate the influence of two soil types (clay loam, sandy loam) on early root development of the grapevine varieties of 'Calardis Musqué', 'Villard Blanc' and V3125 ('Schiava Grossa' x 'Riesling').

Table 1

Soil properties of both soil types (Analysis Report by Tim O'Hare Associates, Soil and Landscape Consultancy)

Soil Properties		
Texture class (UK classification)	Clay loam	Sandy loam
Clay (< 0.002 mm) [%]	24.0	13.0
Silt (0.002 - 0.063 mm) [%]	40.0	15.0
Sand (0.063 - 2.0 mm) [%]	36.0	72.0
pH	6.5	7.9
Organic matter (LOI) [%]	5.1	4.1

Material and Methods

Plant material and cultivation: Dormant, woody cuttings (ca. 10 cm long, carrying two winter buds) of 'Calardis Musqué' (*V*IVC variety number 4549), 'Villard Blanc' (*V*IVC variety number 13081) and Geilweilerhof V. 3125 (*V*IVC variety number 4605) ('Schiava Grossa' x 'Riesling', abbreviation V3125) (www.vivc.de) were placed into Jiffy-7® pellets covered by a plastic sheet and kept in the green house (conditions: 25 °C/20 °C day/night) to initiate root formation. After one week, cuttings were re-planted into polypropylene columns (15 cm height × 7.5 cm diameter). Every column was covered with a mesh at the bottom end to avoid soil loss and water logging. All columns were uniformly packed with air-dried and sieved soil (< 2 mm) of either clay loam or sandy loam (Tab. 1). Afterwards, each column was saturated from the bottom upwards with deionised water and placed in the green house. A randomised order ensured equal treatment of the variants. Three replicates of each genotype 'Calardis Musqué', 'Villard Blanc' and V3125 were planted into each soil type, giving a total of 18 columns. All samples were irrigated daily with deionised water except the day of scanning to prevent overlapping attenuation values of root material and water-filled soil pores, which can interfere subsequent root segmentation.

X-ray µCT scans and reconstruction of 3D models: After six weeks, roots of the biggest root system were already grown through the soil and along the inner wall of the column and therefore, all replicates were scanned at this timepoint. A phoenix v|tome|x m® X-ray µCT scanner (GE Measurement & Control Solutions, Wunsdorf, Germany) was used and columns were placed separately in the scanner chamber. Hereby, scan position and settings were kept constant for each column. The scanning resolution was 42 µm, with 1800 projection images taken per scan. To acquire maximal resolution, each column was scanned in three parts: upper, middle, and lower part of the column. Every scan took approximately 18 min and resulted in an image stack of grey-scale images which were processed immediately after the scan: 3D image reconstruction was performed using the 'multi-scan feature' in *phoenix datos*|x 2.0 software (GE Measurement & Control Solutions, Wunsdorf, Germany) to combine the three individual scans of each column. A beam hardening correction filter setting of 8 was applied. Whole image reconstruction took approximately 10 min per sample.

Reconstruction of 3D model and quantification of root traits: Root systems were segmented from the µCT 3D image data using StudioMax®v2.2 software. By use of the 'Region Growing' selection tool,

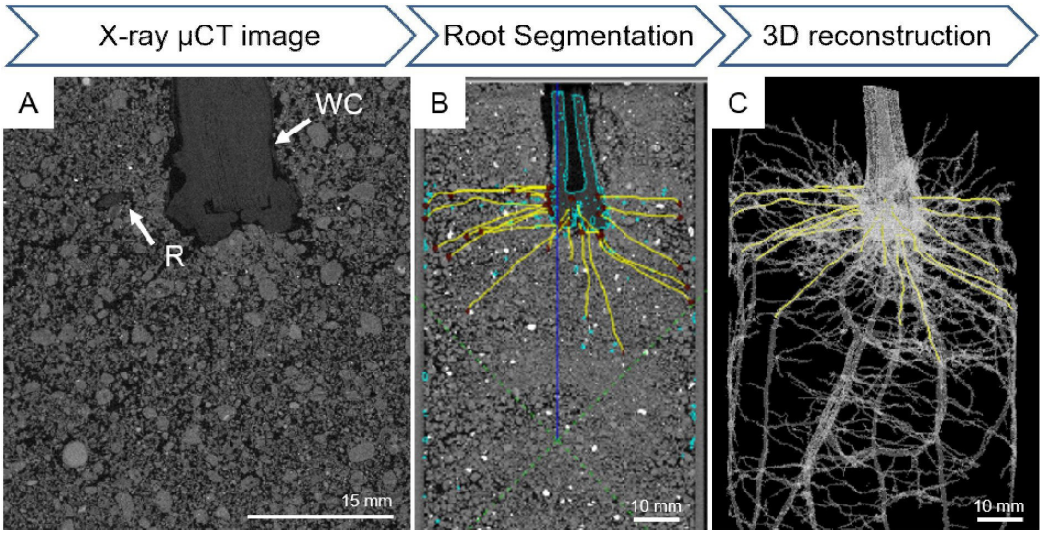

Fig. 1: Workflow from X-ray grey scale image to reconstructed 3D model of the root system. (**A**) µCT image of a vertical slice through the soil column with indicated woody cutting (WC) and root (R). (**B**) Image of advanced stage of the root segmentation process. Stem and roots of the same grey scale range are highlighted in blue (detected by 'Region Growing' selection tool); adventitious roots were traced manually and are indicated in yellow. (**C**) Fully reconstructed 3D model of the root system.

roots were segmented based on differences in gray-scale color intensity between roots, soil, and pore space (Fig. 1). Additionally, the sequential use of an open and then close function in VG StudioMax® was used to fill unselected areas within the root 'region of interest' (ROI) and smooth the boundary of the root surface. Based on the greyscale segmentation along the ROI boundaries, 3D models of the entire root system were reconstructed for quantification of root systems. Stems of the woody cuttings were removed and root volume and root surface area were quantified by the VG StudioMAX® software, taking approximately 1 to 3 d per sample depending on their root system extent. In order to determine number and length of adventitious roots as well as lateral roots, 'Polyline' tool of VG StudioMAX® was used. First, adventitious roots were traced from their origin at the woody cutting towards their tips. Afterwards, lateral roots were traced from their point of branching off from adventitious roots. The resulting lines were measured and counted. Quantification of root number and length took 1 to 5 d per sample mostly depending on the number of lateral roots. In addition, growth angles of adventitious roots emerging from the woody cutting and a horizontal axis were measured with the in-house software RooTrak (Mairhofer *et al.* 2017; Fig. 2).

Statistical analysis: Two-way-ANOVA was conducted to compare the main effects of soil type and genotype as well as their interaction effects on each measured trait (R Studio, Version 3.5.1). Pearson's correlation coefficients were calculated to examine whether single root traits are associated with each other.

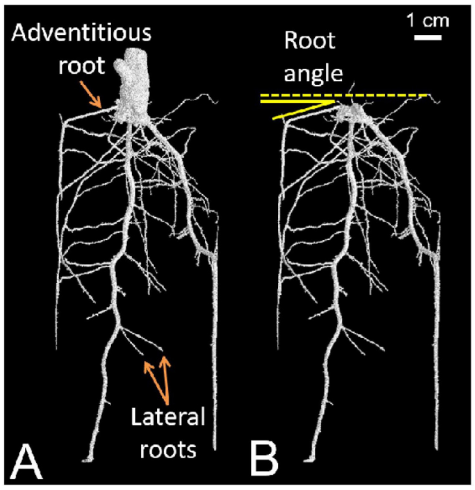

Fig. 2: 3D model of a 'Villard Blanc' root system including the bottom part of the woody cutting. Both root types, adventitious roots emerging from the woody cutting and lateral roots branching off the adventitious roots are indicated (**A**). Woody cutting stem is removed for root quantification and a horizontal axis illustrates the root angle measurement of adventitious roots emerging from the stem (**B**).

Results and Discussion

Evaluation of X-ray µCT for grapevine root system phenotyping: X-ray µCT was successfully applied to acquire non-invasively the entire root system of young grapevine cuttings grown in soil-filled columns. The selected size of the planting columns depended predominantly on the scanner model. For the present study, mid-size columns (15 cm height × 7.5 cm diameter) were used offering an adequate soil space for adventitious root formation. However, roots of 'Calardis Musqué' and V3125 showed strong root growth in clay loam in comparison to sandy loam or 'Villard Blanc' and thus, the roots covered large parts of the soil column. Especially the outer roots had grown sideways along the inner wall of the columns, which do not influence the total root length values but changes the orientation angles of adventitious root growth. Due to the fast and extensive root growth, scans of distinctly older grapevine root systems should be executed in larger columns and scanner models. In comparison to other crops like cereals or rapeseed, the grapevine roots, especially adventitious roots,

are relatively thick and therefore, easier to detect because they are clearly visible on X-ray images. Fine roots of < 0.2 mm would not be visible via µCT at 57.3 µm voxel size (Zappala *et al.* 2013), which could lead to underestimation of root system of crops with very fine roots. In addition, the root segmentation process of thicker roots can be accelerated by using the 'Region Growing' function in VG StudioMax®. This function detects root-like grey scales in the surrounding of already detected roots automatically, which speeds up the very time-consuming and labour-intensive manual root segmentation process.

Reconstruction of 3D models and quantification of root characteristics: The reconstructed 3D models are the basis for the determination of phenotypic root characteristics. The 3D models of all genotypes in both soil types are presented in Fig. 3. Based on these models, quantification of root traits due to length measurements and counting was conducted to identify effects of genotype and soil type as well as their interaction on the root system development. Fig. 4 shows means of all measured traits of all genotypes and both soil types. In general, 'Calardis Musqué' developed more and longer roots than V3125 and V3125 exhibited more and longer roots than 'Villard Blanc'.

The number and length of adventitious roots, total root length and root system surface as well as root system vol-

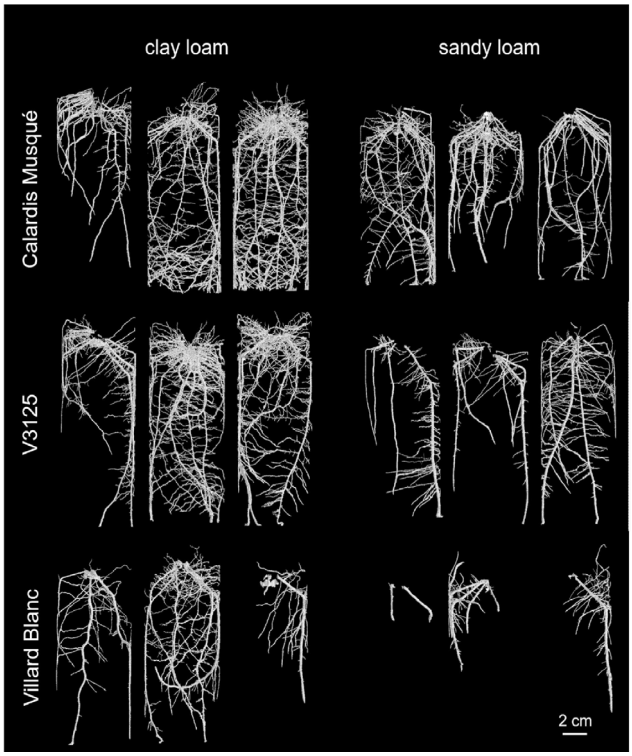

Fig. 3: 3D models of all three genotypes 'Calardis Musqué', V3125, and 'Villard Blanc' in both soil types: clay loam and sandy loam.

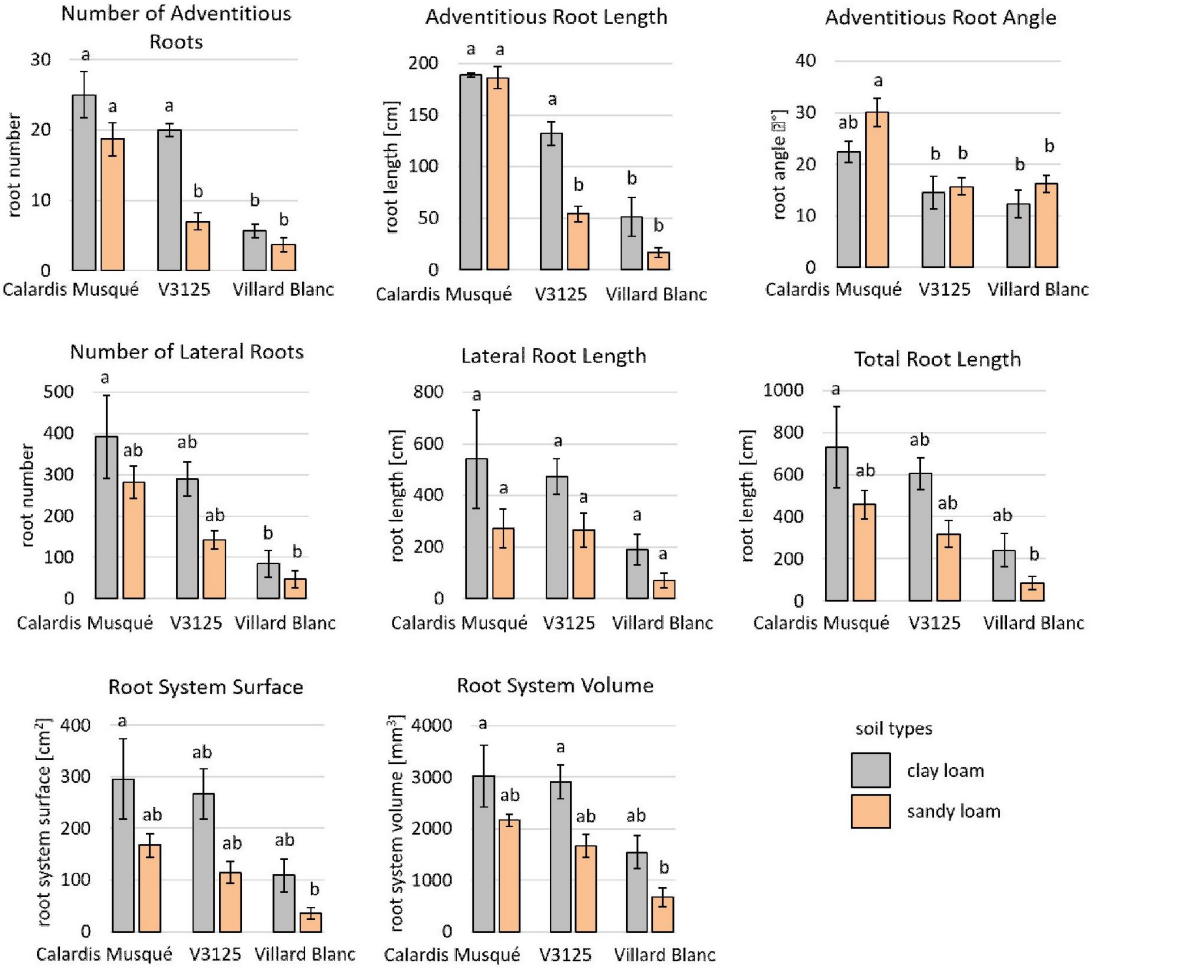

Fig. 4: Means and standard errors of each trait per genotype and soil type (n = 3). Different letters indicate significant differences at $p < 0.05$, tested by two-way ANOVA.

ume were mainly affected by the genotype (63.5 %, 80.9 %, 42.5 %, 33.5 %, and 41.1 % phenotypic variance explained), but also significantly by the soil type (16.4 %, 7.4 %, 18.4 %, 25.6 %, and 24.7 %). Adventitious root length was the only trait exhibiting a significant interaction of both factors with 4.9 % explained variance. Adventitious root angle and number of lateral roots showed only significant phenotypic effects with 56.2 % and 53.6 % explained phenotypic variance each. Lateral root length was neither significantly affected by genotype, soil type nor their interaction. Only for adventitious root length, an interaction of both factors was significant (Tab. 2).

Measuring root system surface and volume was less extensive than acquiring number and length of adventitious and lateral roots. Root system surface and volume highly correlate with lateral root number and length as well as total root length (r = 0.91 to 0.98; see Tab. 3). However, correlation with number of adventitious roots resulted in only r = 0.58 and r = 0.62. Interestingly, adventitious root number showed significant differences between genotypes and soil types which were not confirmed significantly by root system surface or volume. Therefore, the time-consuming process of determining the number of adventitious roots cannot be skipped and replaced by only measuring root system surface or volume. In addition, adventitious root angle was not strongly correlated to the other measured traits, indicating a promising unique trait for further root system analyses. Adventitious root formation of V3125 was significantly

Table 2

Results of two-way ANOVA of measured root traits determining effects of soil type and genotype (n = 3)

Trait	Effect	Df	Mean Sq	F value	*p*-value		Variance explained (%)
Number of Adventitious Roots	Soil Type	1	227.6	14.53	0.0025	**	16.35
	Genotype	2	442.2	28.22	< 0.0000	***	63.53
	Interaction	2	46.1	2.94	0.0914	.	6.62
Adventitious Root Length	Soil Type	1	6570.0	12.89	0.0037	**	7.38
	Genotype	2	35984.0	70.62	< 0.0000	***	80.89
	Interaction	2	2157.0	4.23	0.0407	*	4.85
Adventitious Root Angle	Soil Type	1	80.1	3.16	0.1009		8.42
	Genotype	2	267.8	10.56	0.0023	**	56.23
	Interaction	2	15.7	0.62	0.5543		3.31
Number of Lateral Roots	Soil Type	1	43709.0	3.80	0.0752	.	10.61
	Genotype	2	110442.0	9.59	0.0033	**	53.59
	Interaction	2	4675.0	0.41	0.6752		2.27
Lateral Root Length	Soil Type	1	177661.0	4.31	0.0600	.	18.53
	Genotype	2	1344993.0	3.28	0.0732	.	28.16
	Interaction	2	8384.0	0.20	0.8186		1.75
Total Root Length	Soil Type	1	252562.0	5.84	0.0325	*	18.44
	Genotype	2	291217.0	6.74	0.0109	*	42.53
	Interaction	2	7792.0	0.18	0.8373		1.14
Root System Surface	Soil Type	1	62948.0	7.91	0.0157	*	25.62
	Genotype	2	41123.0	5.17	0.0241	*	33.48
	Interaction	2	2486.0	0.31	0.7374		2.02
Root System Volume	Soil Type	1	4429805.0	8.86	0.0116	*	24.70
	Genotype	2	3682043.0	7.36	0.0082	**	41.06
	Interaction	2	70674.0	0.14	0.8696		0.79

Signif. codes: '***' < 0.001; '**' 0.001 - 0.01; '*' 0.01 - 0.05; '.' 0.05 - 0.1; ' ' 0.1 - 1

Table 3

Correlations between measured traits given as Pearson correlations

Measured Trait	ARN	ARL	ARA	LRN	LRL	TRL	RSS
Adventitious Root Number (ARN)	1.00						
Adventitious Root Length (ARL)	0.90	1.00					
Adventitious Root Angle (ARA)	0.37	0.63	1.00				
Number of Lateral Roots (LRN)	0.63	0.79	0.53	1.00			
Lateral Root Length (LRL)	0.42	0.55	0.27	0.91	1.00		
Total Root Length (TRL)	0.58	0.72	0.39	0.96	0.98	1.00	
Root System Surface (RSS)	0.58	0.68	0.34	0.94	0.97	0.98	1.00
Root System Volume (RSV)	0.62	0.73	0.37	0.93	0.95	0.98	0.98

reduced in sandy loam concerning number and length of adventitious roots. Root systems of 'Calardis Musqué' and 'Villard Blanc' were not significantly affected by the soil type but also tend to evolve smaller root systems in sandy loam.

Comparing the genotypes grown in clay loam with each other, 'Calardis Musqué' and V3125 revealed significantly higher number and length of adventitious roots compared to 'Villard Blanc'. In addition, 'Calardis Musqué' had significantly more lateral roots than 'Villard Blanc'. Differences between the genotypes became more evident comparing the three genotypes grown in sandy loam. Significantly greater root systems of 'Calardis Musqué' were found compared to V3125 and 'Villard Blanc' regarding number and length of adventitious roots as well as adventitious root angle. These findings indicate that genotypic differences between 'Calardis Musqué' and 'Villard Blanc' are strengthened by sandy loam soil conditions, especially for V3125. Whereas, there were no significant differences between 'Calardis Musqué' and V3125 in clay loam, 'Calardis Musqué samples showed significantly more and longer adventitious roots in sandy loam.

In general, 'Calardis Musqué', V3125 and 'Villard Blanc' developed broader root systems in clay loam compared to sandy loam, especially V3125 showed a decreased number and length of adventitious roots in sandy loam. As a consequence, the drier sandy soil possibly possess increased penetration resistance resulting in a greater physical impediment to root growth (Soar and Loveys 2007). Studying root systems of wheat, pea and tomato by X-ray µCT revealed comparable results of increased convex hull area and root thickness in clay loam compared to loamy sand (Helliwell *et al.* 2019). Interestingly, observations on older vines in vineyards showed similar effects: Investigation of root density in a field study by trenching demonstrated that the available water supply had a positive effect, whereas hydromorphy intensity and penetrometer soil strength had a negative influence on vine rooting (Morlat and Jacquet 1993). In addition, it is known that large proportions of sand fragments (0.06-2 mm) in vineyard soils cause poor water retention capacity and low fertility (White 2015) because the water moves below the root system and takes away soluble nutrients (Peacock 1996).

Initial adventitious root formation from woody cuttings is regulated by genetic factors, soil temperature as well as by other internal compounds like phytohormones or available carbohydrates (Haissig *et al.* 1992, Friend *et al.* 1994, Smart *et al.* 2003). Several studies have identified differences in root systems among different grapevine genotypes e.g. in terms of root distribution observed by soil coring of a trench profile (Perry *et al.* 1983) or regarding root density (Williams and Smith 1991) analyzed in an excavation trial within a given edaphic environment. In our experiment, genotypic effects on root formation could be determined non-invasively with measurements of whole intact root systems. An early grapevine study (Guillon 1905) indicated that different geotropic angles of adventitious roots result in variations of the vertical and horizontal depth distributions. In contrast, a compilation of more recent data suggested emergence angles from stem cuttings may not be a good indicator of the depth distribution of roots (reviewed by Smart *et al.* 2006). Even though X-ray µCT was successfully used for phenotyping of grapevine root systems, the low-throughput method is limited due to financial costs but also because of a time-consuming process of root system reconstruction from X-ray images. Therefore, a use for breeding purposes (e.g. screening of whole crossing populations with many individuals and an appropriate number of replications) seems rather unlikely at present. However, with proving the general suitability of grapevine woody cuttings for X-ray µCT, other fields of research could benefit from this technique. For instance, the quantification of nodosities on grapevine roots induced by phylloxera is challenging and highly invasive for potted plants, because the roots have to be made accessible for assessment by washing them out of the soil. A non-invasive technique like X-ray µCT could bring new insights into this field.

Conclusion

In the present study, the technique of non-invasive, high-resolution X-ray µCT and subsequent reconstruction of 3D models was successfully applied on young grapevine woody cuttings in order to acquire an accurate 3D visualisation of the whole, intact root system. Based on the generated 3D models, automated measurements of the early root system development, *i.e.* number and length of adventitious and lateral root formation was feasible. The obtained results indicated (i) genotypic differences between root architectural traits of 'Calardis Musqué' and 'Villard Blanc'; and (ii) soil type affected adventitious root formation probably due to variation in water supply and physical penetration resistance of sandy loam. The technique enables new insights into the accurate 3D structure and extends the knowledge of 3D growth parameters of young grapevine root systems, e.g. relation of adventitious and lateral roots and branching. An important application could be the investigation of the root response to drought stress or soil limestone, the objective comparison of the roots of grapevine varieties as well as gaining new insights about phylloxera root infection.

Acknowledgements

Financial support by the Access to Research Infrastructures activity in the Horizon2020 Programme of the EU (EPPN2020 Grant Agreement 731013) is gratefully acknowledged. Further, we also thank R. Wehrle (University of Bonn, Soil Research) for the discussion about soil properties.

References

Atkinson, J. A.; Pound, M. P.; Bennett, M. J.; Wells, D. M.; 2019: Uncovering the hidden half of plants using new advances in root phenotyping. Curr. Opin. Biotechnol. **55**, 1-8. DOI: https://doi.org/10.1016/j.copbio.2018.06.002

Battista, F.; Gaiotti, F.; Bragato, G.; Tomasi, D.; 2016: Root system distribution and density of 'Pinot Gris': effect on yield and grape quality. Proc. I. Int. Symp. Grapevine Roots, Acta Hortic. (ISHS) **1136**, 109-114. DOI: https://doi.org/10.17660/ActaHortic.2016.1136.15

Delrot, S.; Grimplet, J.; Carbonell-Bejerano, P.; Schwandner, A.; Bert, P. F.; Bavaresco, L.; Dalla Costa, L.; Di Gaspero, G.; Duchêne, E.;

Hausmann, L.; Malnoy, M.; Morgante, M.; Ollat, N.; Pecile, M.; Vezzulli, S.; 2020: Genetic and genomic approaches for adaptation of grapevine to climate change, 157-270. In: C. Kole (Ed.): Genomic designing of climate-smart fruit crops. Springer Nature, Cham, Switzerland. DOI: https://doi.org/10.1007/978-3-319-97946-5_7

Friend, A. L.; Coleman, M. D.; Isebrands, J. G.; 1994: Carbon allocation to root and shoot systems of woody plants, 245-274. In: T. D. Davis, B. E. Haissig (Eds): Biology of adventitious root formation. Plenum Press, London and New York. DOI: https://doi.org/10.1007/978-1-4757-9492-2_18

Guillon, J. M.; 1905: Étude Générale de la Vigne: Historique les Vignobles et les Crus Anatomie et Physiologie, Sol et Climat. Masson, Paris.

Haissig, B. E.; Davis, T. D.; Riemenschneider, D. E.; 1992: Researching the controls of adventitious rooting. Physiol. Plant. **84**, 310-317. DOI: https://doi.org/10.1111/j.1399-3054.1992.tb04669.x

Helliwell, J. R.; Sturrock, C. J.; Miller, A. J.; Whalley, W. R.; Mooney, S. J.; 2019: The role of plant species and soil condition in the structural development of the rhizosphere. Plant Cell Environ. **42**, 1974-1986. DOI: https://doi.org/10.1111/pce.13529

Jahnke, S.; Menzel, M. I.; van Dusschoten, D.; Roeb, G.W.; Bühler, J.; Minwuyelet, S.; Blümler, P.; Temperton, V. M.; Hombach, T.; Streun, M.; 2009: Combined MRI-PET dessects dynamic changes in plant structures and functions. Plant J. Cell Mol. Biol. **59**, 634-644. DOI: https://doi.org/10.1111/j.1365-313X.2009.03888.x

Mairhofer, S.; Pridmore, T.; Johnson, J.; Wells, D.M.; Bennett, M.J.; Mooney, S.J.; Sturrock, C.J.; 2017: X-ray Computed Tomography of crop plant root systems grown in soil. Curr. Protoc. Plant Biol. **2**, 270-286. DOI: https://doi.org/10.1002/cppb.20049

Mairhofer, S.; Sturrock, C. J.; Bennett, M. J.; Mooney, S. J.; Pridmore, T. P.; 2015: Extracting multiple interacting root systems using X-ray microcomputed tomography. Plant J. **84**, 1034-1043. DOI: https://doi.org/10.1111/tpj.13047

Metzner, R.; van Dusschoten, D.; Bühler, J.; Schurr, U.; Jahnke, S.; 2014: Belowground plant development measured with magnetic resonance imaging (MRI): exploiting the potential for non-invasive trait quantification using sugar beet as a proxy. Front. Plant Sci. **5**, art. 469. DOI: https://doi.org/10.3389/fpls.2014.00469

Morlat, R.; Jacquet, A.; 1993: The soil effects on the grapevine root system in several vineyards of the Loire valley, France. Vitis **32**, 35-42. DOI: https://doi.org/10.5073/vitis.1993.32.35-42

Peacock, B.; 1996: Potassium in Soils and Grapevine Nutrition. Pub. NG9-99, University of California (https://ucanr.edu/sites/Tulare_County/files/82033.pdf).

Perry, R. L.; Lyda, S. D.; Bowen, H. H.; 1983: Root distribution of four *Vitis* cultivars. Plant Soil **71**, 63-74. DOI: https://doi.org/10.1007/978-94-009-6833-2_7

Rogers, E. D.; Monaenkova, D.; Mijar, M.; Nori, A.; Goldman, D. I.; Benfey, P.N.; 2016: X-Ray Computed Tomography reveals the response of root system architecture to soil texture. Plant Physiol. **171**, 2028-2040. DOI: https://doi.org/10.1104/pp.16.00397

Smart, D. R.; Kocsis, L.; Walker, M. A.; Stockert, C.; 2003: Dormant buds and adventitious root formation by *Vitis* and other woody plants. J. Plant Growth Regul. **21**, 296-314. DOI: https://doi.org/10.1007/s00344-003-0001-3

Smart, D. R.; Schwass, E.; Lakso, A.; Morano, L.; 2006: Grapevine rooting patterns: a comprehensive analysis and a review. Am. J. Enol. Vitic. **57**, 89-104 (https://www.ajevonline.org/content/57/1/89).

Soar, C. J.; Loveys, B. R.; 2007: The effect of changing patterns in soil-moisture availability on grapevine root distribution, and viticultural implications for converting full-cover irrigation into a point-source irrigation system. Aust. J. Grape Wine Res. **13**, 2-13. DOI: https://doi.org/10.1111/j.1755-0238.2007.tb00066.x

Tracy, S. R.; Black, C. R.; Roberts, J. A.; Sturrock, C.; Mairhofer, S.; Craigon, J.; Mooney, S. J.; 2012: Quantifying the impact of soil compaction on root system architecture in tomato (*Solanum lycopersicum*) by X-ray micro-computed tomography. Ann. Bot. **110**, 511-519. DOI: https://doi.org/10.1093/aob/mcs031

White, R. E.; 2015: Understanding Vineyard Soils. Oxford University Press, 2nd edition (https://global.oup.com/academic/product/understanding-vineyard-soils-9780199342068?cc=de&lang=en&).

Williams, L. E.; Smith, R. J.; 1991: The effect of rootstock on the portioning of dry weight, nitrogen and potassium, and root distribution of Cabernet Sauvignon grapevines. Am. J. Enol. Vitic. **42**, 118-122 (https://www.ajevonline.org/content/42/2/118).

Zappala, S.; Mairhofer, S.; Tracy, S.; Sturrock, C. J.; Bennett, M.; Pridmore, T.; Mooney, S.; 2013: Quantifying the effect of soil moisture content on segmenting root system architecture in X-ray computed tomography images. Plant Soil **370**, 35-46. DOI: https://doi.org/10.1007/s11104-013-1596-1

Received July 23, 2020
Accepted November 11, 2020